



Neuropharmacology and analgesia

A novel radioligand for the ATP-gated ion channel P2X7: [³H] JNJ-54232334

Brian Lord^{a,*}, Michael K. Ameriks^a, Qi Wang^a, Lawrence Fourgeaud^a, Maarten Vliegen^b, Willy Verluyten^b, Pieter Haspeslagh^b, Nicholas I. Carruthers^a, Timothy W. Lovenberg^a, Pascal Bonaventure^a, Michael A. Letavic^a, Anindya Bhattacharya^a

^a Janssen Research & Development, LLC, Neuroscience Drug Discovery, 3210 Merryfield Row, San Diego, CA 92121-1126, United States

^b Janssen Research & Development, LLC, Drug Safety Sciences, Turnhoutseweg 30, Beerse 2340, Belgium

ARTICLE INFO

Article history:

Received 5 June 2015

Received in revised form

14 September 2015

Accepted 15 September 2015

Available online 18 September 2015

Keywords:

P2X7

Radioligand binding

Depression

Autoradiography

Receptor occupancy

JNJ-54232334

JNJ-54140515

ABSTRACT

The ATP-gated ion channel P2X7 has emerged as a potential central nervous system (CNS) drug target based on the hypotheses that pro-inflammatory cytokines such as IL-1 β that are released by microglia, may contribute to the etiology of various disorders of the CNS including depression. In this study, we identified two closely related P2X7 antagonists, JNJ-54232334 and JNJ-54140515, and then tritium labeled the former to produce a new radioligand for P2X7. JNJ-54232334 is a high affinity ligand for the rat P2X7 with a pK_i of 9.3 \pm 0.1. In rat cortical membranes, [³H] JNJ-54232334 reached saturable binding with equilibrium dissociation (K_d) constant of 4.9 \pm 1.3 nM. The compound displayed monophasic association and dissociation kinetics with fast on and off rates. In rat brain sections, specific binding of [³H] JNJ-54232334 was markedly improved compared to the previously described P2X7 radioligand, [³H] A-804598. In P2X7 knockout mouse brain sections, [³H] A-804598 bound to non-P2X7 binding sites in contrast to [³H] JNJ-54232334. In rat or wild type mouse brain sections [³H] JNJ-54232334 bound in a more homogenous and region independent manner. The ubiquitous expression of P2X7 receptors was confirmed with immunohistochemistry in rat brain sections. The partial displacement of [³H] A-804598 binding resulted in the underestimation of the level of ex vivo P2X7 occupancy for JNJ-54140515. Higher levels of P2X7 ex vivo occupancy were measured using [³H] JNJ-54232334 due to less non-specific binding. In summary, we describe [³H] JNJ-54232334 as a novel P2X7 radioligand, with improved properties over [³H] A-804598.

© 2015 Elsevier B.V. All rights reserved.

1. Introduction

P2X7 receptors are ligand gated ion channels that are activated by ATP (Bartlett et al., 2014). ATP-induced activation of the P2X7 ion channel causes opening of the channel pore leading to subsequent flux of non-selective cations such as calcium, sodium and potassium (Chataigneau et al., 2013). A hallmark feature of P2X7 activation is the subsequent activation of the NLRP3 inflammasome leading to release of the pro-inflammatory cytokine IL-1 β (Iwata et al., 2013; Solle et al., 2001). P2X7 has emerged as a potential CNS drug target based on the hypotheses that pro-inflammatory cytokines such as IL-1 β released by microglia, where P2X7 is abundantly expressed, may contribute to the etiology of various disorders of the CNS (Chrovian et al., 2014; Sperlagh and

Illes, 2014). Several reports have emerged recently describing novel chemical entities that target the brain P2X7 ion channel (Abdi et al., 2010; Bhattacharya et al., 2013; Gao et al., 2015; Letavic et al., 2013; Lord et al., 2014; Rudolph et al., 2015; Savall et al., 2015; Wilkinson et al., 2014).

There is growing evidence that P2X7 may play a role in the pathology of depression (Ortiz et al., 2015; Sperlagh et al., 2012; Stokes et al., 2015); both unipolar and bipolar. P2X7 knockout mice are protected from depressogenic behaviors according to multiple reports (Basso et al., 2009; Boucher et al., 2011; Csolle et al., 2013a) and in line with these data, pharmacological blockade of P2X7 also lead to antidepressant like effects (Csolle et al., 2013b; Wilkinson et al., 2014). Moreover, the role of IL-1 β signaling in the brain in animal models of depression that are induced by chronic stress mediated deficits of hedonic behavior have strengthened the P2X7 IL-1 β axis in the context of depression (Goshen et al., 2008; Koo and Duman, 2008; Zhang et al., 2015). Emerging data also suggest the potential benefit of P2X7 antagonists in managing bipolar disorder (Bhattacharya et al., 2013; Csolle et al., 2013a; Gubert

* Correspondence to: Janssen Research & Development, LLC, Neuroscience Therapeutic Area, 3210 Merryfield Row, San Diego, CA 92121, United States. Fax: +1 858 784 3085.

E-mail address: blord@its.jnj.com (B. Lord).

et al., 2014).

High affinity and selective radioligands are used in drug discovery programs to define binding affinity of compounds under true equilibrium where complete displacement is achieved, or in cases of partial or no displacement, a radioligand can reveal alternate binding pockets. In addition, radioligands are also used to determine the *ex vivo* receptor occupancy of central P2X7 receptors after peripheral administration of drugs (Able et al., 2011; Bhattacharya et al., 2013; Lord et al., 2014). [³H] A-804598 (2-Cyano-1-(1-phenylethyl)-3-quinolin-5-ylguanidine) is the first and only radioligand described to date for P2X7 (Donnelly-Roberts et al., 2009). However, we observed higher than optimal non-specific binding and lack of complete displacement in rat brains but not in cells expressing the recombinant rat P2X7 channel. We focused on identifying a second generation P2X7 radiotracer and we describe [³H] JNJ-54232334 (7-[2-Chloro-3-(trifluoromethyl)benzyl]-6-methyl-3-pyrimidin-2-yl-6,7-dihydro[1,2,4]triazolo[4,3-a]pyrazin-8(5H)-one), as a novel P2X7 radioligand.

2. Materials and methods

All animal work described in this paper was done in accordance with the Guide Care for and Use of Laboratory Animals adopted by the US National Institutes of Health. Animals were allowed to acclimate for 7 days after receipt. They were group housed in accordance with institutional standards, received food and water *ad libitum* and were maintained on a 12 h light/dark cycle.

2.1. *In vitro* P2X7 pharmacology

The calcium flux assay and the radioligand binding assay were used to define the potency and affinity of JNJ-54232334 and JNJ-54140515, respectively. Bz-ATP was used to stimulate P2X7 in functional assays and [³H] A-804598 was used as the radioligand of choice to measure the affinity of JNJ-54232334 at the recombinant rat P2X7 membranes whereas [³H] A-804598 and [³H] JNJ-54232334 were both used in rat brain homogenates. For calcium flux assay, 1321N1 cells expressing P2X7 orthologues were dissociated 18–24 h prior to the assay using 0.05% trypsin/EDTA (Invitrogen, Grand Island, NY, USA), and plated at density of 25,000 cells well⁻¹ into poly-D-lysine coated 96-well black-walled clear bottom plates (Becton-Dickinson, Bedford, MA, USA). On the day of the experiment, cells were washed with assay buffer, containing (in mM): 130 NaCl, 2 KCl, 1 CaCl₂, 1 MgCl₂, 10 HEPES, 5 glucose; pH 7.4 and dye loaded with a 2 × Calcium-4 (Molecular Devices, Sunnyvale, CA, USA). Cells were stained with the Calcium-4 dye in staining buffer for 30 min at room temperature in the dark. Test compounds were prepared at 250 × the final test concentration in neat dimethylsulfoxide. Intermediate 96-well compound plates were prepared by transferring 1.2 μL of the compound into 300 μL of assay buffer. A further 3 × dilution occurred when transferring 50 μL well⁻¹ of the compound plate to 100 μL well⁻¹ in the cell plate. Cells were incubated with test compounds and dye for 30 min. Calcium flux was monitored in Fluorescence Imaging Plate reader (FLIPR^{Tetra}) as the cells were challenged by adding 50 μL well⁻¹ of BzATP. The final concentration of Bz-ATP was 250 μM. Experiments were run in triplicate with antagonistic potency values calculated in GraphPad Prism Software version 5.0 (San Diego, CA) and expressed as pIC₅₀.

For radioligand binding with Sprague Dawley rat cortex, tissues were homogenized followed by high-speed centrifugation (32,000 g) of the supernatants for 30 min. The membrane pellet was then re-suspended in ice cold assay buffer (Tris-HCl+0.1% BSA) so that the final concentration of membrane was 400 μg/well. For association and dissociation experiments, a fixed

concentration of the radioligand was either associated with increasing time of incubation or dissociated with an excess of a competitor (A-804598; 1 μM). For the association study, two concentrations of tracer (close to K_d and $2K_d$) were incubated with increasing time (1, 5, 10, 15, 20, 30, 40, 60 and 120 min) with membranes in volumes of 40 μL (tracer), 50 μL (membrane) and 10 μL (buffer). For the dissociation study, the total incubation volume was 290 μL (40 μL tracer; 50 μL membrane; 200 μL A-804598; 1 μM); dissociation was initiated by adding an excess of (200 μL) A-804598 (1 μM) at different time points (240, 210, 180, 150, 120, 105, 90, 75, 60, 55, 50, 45, 40, 35, 30, 25, 20, 15, 10, 5, 2 and 1 min) after a 2 h incubation with tracer and membrane alone. For displacement binding, increasing concentrations of the cold ligand were added to the tracer and membrane in a 100 μL (10 μL cold ligand+40 μL tracer+50 μL membrane suspension) total volume for an incubation time of 1 h. In all cases, the experiment was terminated by filtration (GF/B filters pre-soaked with 0.3% PEI) and washed with washing buffer (Tris-HCl 50 mM) followed by drying the plate for 30–40 min. Radioactivity was read in TopCount (Perkin Elmer) by adding MicroScint 0 in each well. Data are from a single experiment with 4 replicates per data point. Radioligand binding parameters (K_d , B_{max} , K_{on} , K_{off}) were calculated in Graph Prism Software version 5.0. All data are presented as mean ± S.E. M. unless otherwise stated.

2.2. *In vitro* receptor binding autoradiography in rat, wild-type and P2X7 knockout brain sections

Three naïve male Sprague Dawley Rats (approximately 400 g in body weight, Harlan Laboratories Livermore, California, USA), 3 naïve C57/bl6 wild-type (WT) mice and 3 P2X7 knockout (KO) mice (Solle et al., 2001) (8–12 weeks, Jackson Labs, Bar Harbor, Maine, USA) were euthanized by CO₂ asphyxiation. Brains were rapidly frozen on powdered dry ice and stored at –80 °C before sectioning. Tissue sections at the level of the hippocampus of 20 μm thickness were prepared for autoradiography as previously described (Langlois et al., 2001). The sections were kept at –80 °C until use. Briefly, sections were pre-incubated for 15 min at room temperature in 50 mM Tris HCl with 0.1% BSA and then incubated for 1 h in fresh 50 mM Tris HCl, 0.1% BSA supplemented with [³H] A-804598 (30 nM) or [³H] JNJ-54232334 (10 nM). The non-specific binding was determined using adjacent sections incubated in the presence of 100 μM ([³H] A-804598) or 10 μM ([³H] JNJ-54232334) A-740003 (N-[1-[(Cyanoamino)(5-quinolinylamino)methylene]amino]-2,2-dimethylpropyl]-3,4-dimethoxybenzeneacetamide). At the end of the incubation, sections were washed 4 times (5 min each) in ice cold buffer followed by 2 dips in deionized water and rapidly dry under a stream of cold air. Digitized images were acquired with the TRacer β-Imager following a 3 h acquisition with beta acquisition software version 9.4 and high resolution images were acquired with the Dfine β-Imager following 96 h session with beta D acquisition software (Biospaciab, Paris, France)

2.3. *Ex vivo* receptor autoradiography in rat brain sections

Male Sprague Dawley Rats approximately 400 g in body weight, Harlan Laboratories were used. JNJ-54140515 was formulated in 20% Hydroxypropyl-β-Cyclodextrin and delivered in a volume of 5 ml/kg for p.o. dosing and 1 ml/kg for s.c. dosing. For the 10 mg/kg s.c. time course experiment, three animals per time point were used with a time course of 0.25, 0.5, 1, 2, 4, 6, and 24 h post dose. Three animals per dose were used for the p.o. dose dependent receptor occupancy experiment with doses of 0.01, 0.03, 0.1, 0.3, 1, 3, 10, 30 mg/kg with tissue taken 0.5 h post dose.

Ex vivo receptor binding was performed as described in the in

vitro autoradiography section but with the following modification: the sections were not washed before incubation and were incubated 10 min with [^3H] A-804598 or 1 min [^3H] JNJ-54232334. Digitized images were analyzed with M3 Vision (BiospaciLab, Paris, France) software and the whole brain section of each animal was quantified to determine the percent of occupied P2X7 receptors. Ex vivo receptor labeling was expressed as the percentage of receptor labeling in corresponding brain areas of naïve control animals. The percentage of receptor occupancy was plotted against dose or against time using GraphPad Prism 5 (San Diego, CA USA). All data are presented as mean \pm S.E.M. unless otherwise stated.

2.4. Immunohistochemistry

Naïve adult male Sprague Dawley Rats were perfused with 4% PFA in PBS. Brains were dissected out, cryo-protected in 30% sucrose and cut into 20 μm frozen sections mounted onto slides. Antigen retrieval was performed using Target Retrieval Solution (DAKO) according to manufacturer's protocol and nonspecific binding was blocked by incubating sections for 1 h in blocking buffer (0.1% Tween-20, 5% donkey serum and 2% IgG-free BSA in PBS). Sections were then incubated for 48 h at 4 $^{\circ}\text{C}$ with anti-P2X7 (Alomone) and anti-Iba1 (Abcam) in blocking buffer. The data sheet shows nice specificity of the anti-P2X7 antibody by western blot using samples from P2X7 knock out animals as a negative control. After 4 washes in PBS 0.1% Tween-20, sections were incubated for 2 h at 22–24 $^{\circ}\text{C}$ in the dark with Hoechst and fluorophore-coupled secondary antibodies (Jackson) in blocking buffer. Following 4 washes in PBS 0.1% Tween-20, sections were sealed with Fluoromount-G (SouthernBiotech) and stored at 4 $^{\circ}\text{C}$. Images were acquired using a Zeiss LSM 710 microscope and displayed images are maximum projection of z-stacks.

2.5. Drugs and materials

[^3H] A-804598 (18.8 Ci/mmol) was synthesized at Moravex Biochemicals, Inc. (Brea, California, USA). [^3H] JNJ-54232334 (25.6 Ci/mmol) and JNJ-54140515 (7-[2-Chloro-3-(trifluoromethyl)benzyl]-6-methyl-3-pyrazin-2-yl-6,7-dihydro[1,2,4]triazolo[4,3-a]pyrazin-8(5H)-one) were synthesized at Janssen Research & Development, LLC using procedures described in US2014/0275096.

A-740003 was purchased from Tocris Bioscience (Bristol, United Kingdom). Tris HCl, and Hydroxypropyl- β -Cyclodextrin were purchased from Sigma-Aldrich Corporation (St. Louis, Missouri, USA).

3. Results

The chemical structures of the compounds used in this study ([^3H] A-804598, [^3H] JNJ-54232334, A-740003 and JNJ-54140515) are shown in Fig. 1.

3.1. In vitro pharmacology of JNJ-54232334

JNJ-54232334 is a functional antagonist of the human P2X7 ion channel. The potency (pIC_{50}) of the compound to block Bz-ATP induced calcium flux in hP2X7-1321N1 cells was 9.5 ± 0.02 (mean \pm S.E.M.). The potency of JNJ-54232334 for the recombinant rat orthologue was lower than that observed at the hP2X7; the potency at the rP2X7 was 7.5 ± 0.02 (mean \pm S.E.M.). Since functional antagonism is directly dependent to the agonist concentration for compounds binding to the same site as the agonist, and can under-estimate the true affinity, we sought to assess the equilibrium binding affinity of JNJ-54232334 at the rP2X7 using [^3H] A-804598 as the probe radioligand. These experiments showed that JNJ-54232334 is a high affinity compound, causing complete displacement of [^3H] A-804598, with a pK_i of 9.3 ± 0.1 at the rP2X7 (Fig. 2). In this study we have also used JNJ-54140515, which is a close structural analog of JNJ-54232334. The in vitro pharmacology of JNJ-54140515 was comparable to JNJ-54232334; affinity for the rP2X7 was 8.9 ± 0.01 (mean \pm S.E.M.), and potency at the rP2X7 for blocking calcium flux was 7.1 ± 0.3 (mean \pm S.E.M.). Since JNJ-54232334 displayed sub-nanomolar affinity, the next goal was to label the compound with tritium in an effort to prepare a second generation tracer for P2X7 with potentially improved properties over [^3H] A-804598. The flow-scheme utilized to prepare [^3H] to JNJ-54232334 is shown in Fig. 3.

3.2. Characterization of [^3H] JNJ-54232334 in rat brain homogenate and rodent tissue sections

The first step in characterization of [^3H] JNJ-54232334 was to

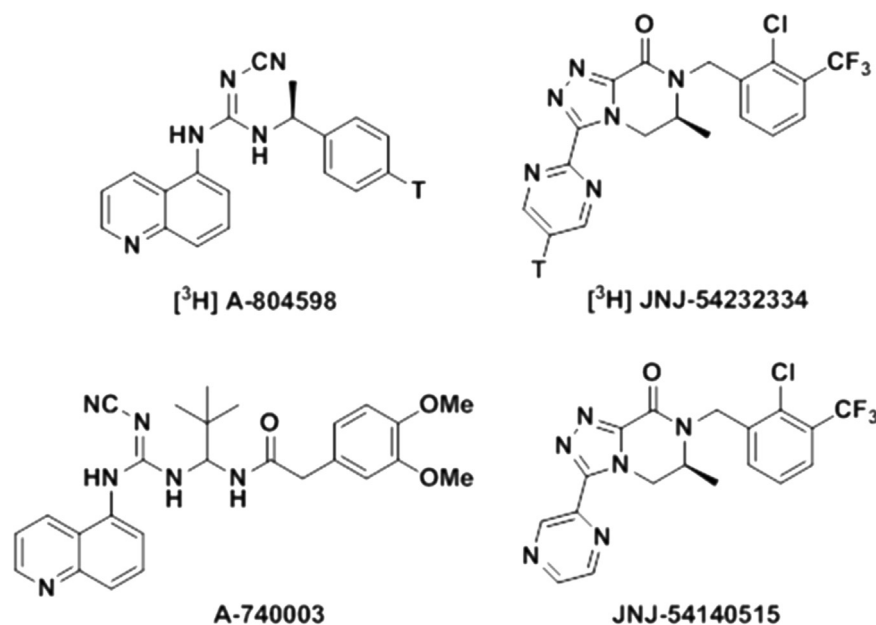


Fig. 1. Chemical structures of [^3H] A-804598, [^3H] JNJ-54232334, A-740003 and JNJ-54140515.

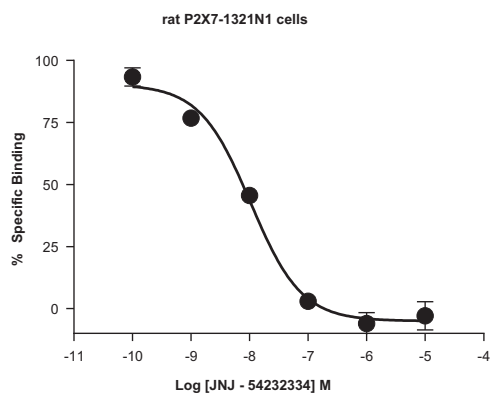


Fig. 2. Equilibrium binding affinity of JNJ-54232334 at the rP2X7 expressed in 1321N1 cells using [^3H] A-804598 as the radioligand. Mean IC_{50} obtained from the experiment was used to determine the affinity (pK_i) using the Cheng-Prusoff correction factor. Data are expressed as mean \pm S.E.M. from three independent experiments in duplicate (each symbol is a mean of 6 data points).

assess the binding isotherm in rat brain homogenates. As displayed in Fig. 4, [^3H] JNJ-54232334 demonstrated concentration dependent binding to rat cortical membranes (Fig. 4A), with a saturable specific binding window (Fig. 4B). Non-specific binding in the assay was determined by 10 μM A-804598. Specific binding of [^3H] JNJ-54232334 reached saturable binding (B_{max}) of approximately 350 fmol/mg protein; the equilibrium dissociation (K_d) constant was 4.9 ± 1.3 nM with a Hill slope of unity. Binding kinetics of [^3H] JNJ-54232334 was also studied using rat cortical membranes. As shown in Fig. 4C, the radioligand associated with the membrane in a concentration and time-dependent manner with on-rate (K_{on}) of $1.18 \times 10^7 \text{ M}^{-1}\text{min}^{-1}$. Likewise, the radioligand displayed monophasic dissociation (Fig. 4D) with a half-time dissociation ($t_{1/2}$) of approximately 22.7 min (95% confidence

interval of 19.7–26.6). This equates to a K_{off} of 0.038 ± 0.002 ($K_{\text{off}} = 0.693/t_{1/2}$). Affinity estimates (K_i) from the kinetic experiment was approximately 3.2 nM, similar to the parameter obtained from saturation binding (4.9 nM).

The next aim was to compare the ability of P2X7 ligands to displace [^3H] JNJ-54232334 and to compare that to the displacement of [^3H] A-804598 in rat brain homogenates or brain sections (Fig. 5). As depicted in Fig. 5A, JNJ-54232334 displaced the binding of [^3H] JNJ-54232334 in a concentration dependent manner. In addition, the displacement was complete at concentrations of 1 μM and above of JNJ-54232334. Contrary to this, when [^3H] A-804598 was used as the radioligand, JNJ-54232334 was not able to displace the radioactivity completely at 10 μM . Lack of complete displacement reached saturation, leaving a significant amount of non-displaceable [^3H] A-804598 binding. This phenomenon was observed with P2X7 ligands across various chemical classes (data not shown), indicating a pharmacology related to [^3H] A-804598 rather than of JNJ-54232334. Interestingly, the potency of JNJ-54232334 was identical ($\text{pIC}_{50} = 7.8 \pm 0.05$) independent of whether [^3H] JNJ-54232334 or [^3H] A-804598 was used as the radioligands, suggesting that the pharmacology of JNJ-54232334 is mediated by P2X7. The inability of JNJ-54232334 to completely displace the [^3H] A-804598 binding suggests that A-804598 is binding to non-P2X7 sites within the brain. To determine if A-804598 binds to a non-P2X7 site in the brain, we tested another potent P2X7 compound, JNJ-54140515. JNJ-54140515 displaced the binding of [^3H] JNJ-54232334 completely, whereas it exhibited partial displacement of [^3H] A-804598, similar to that described in Fig. 5A. In vitro autoradiography was also carried out with both [^3H] A-804598 and [^3H] JNJ-54232334, this time in naïve hippocampal tissue sections following 1 h incubation (Fig. 5B). JNJ-54140515 displaces [^3H] JNJ-54232334 completely but again fails to completely displace binding of [^3H] A-804598. A representative image of the binding of both tracers is shown in Fig. 6

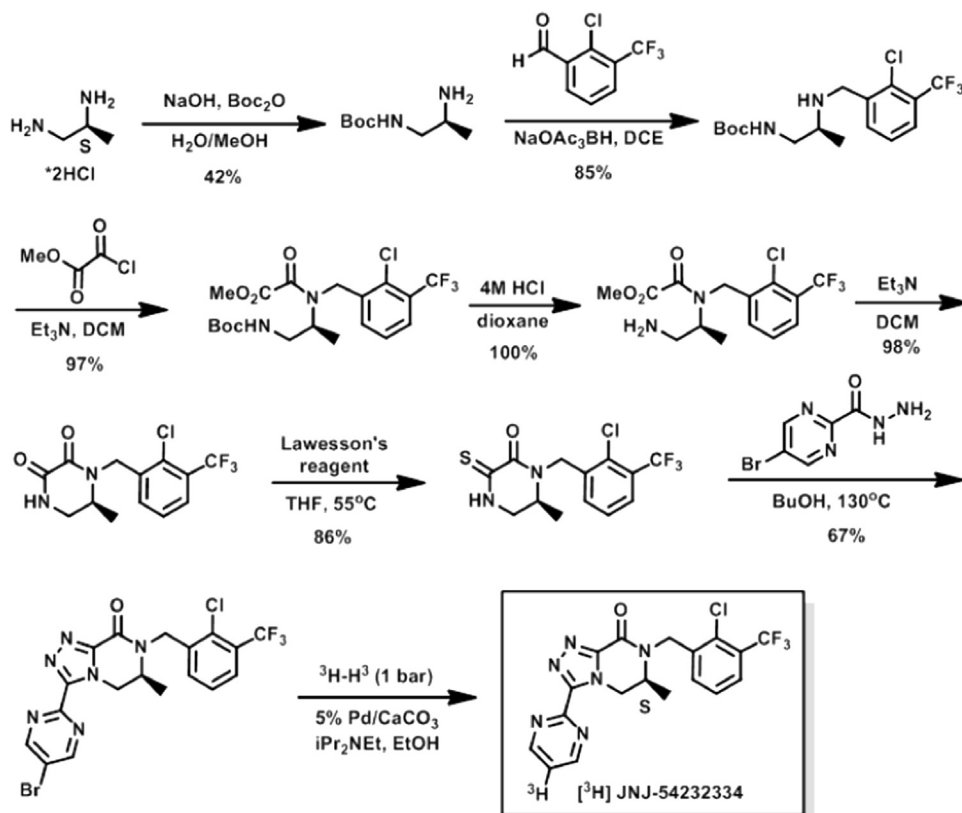


Fig. 3. Radiochemical synthesis of [^3H] JNJ-54232334.

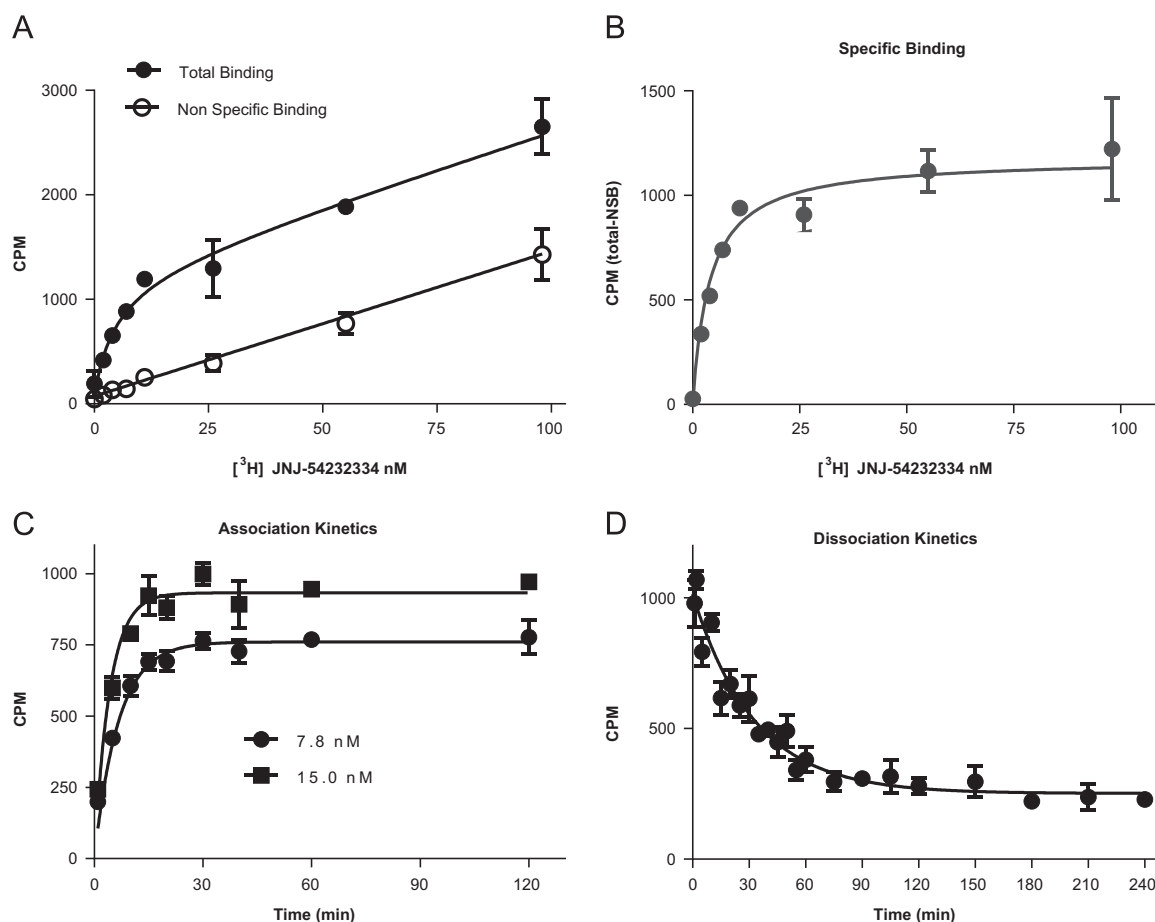


Fig. 4. Saturation binding $[^3\text{H}]$ JNJ-54232334 in rat cortex homogenates. $[^3\text{H}]$ JNJ-54232334 demonstrated concentration dependent binding to rat cortical membranes (A), with a saturable specific binding window (B). Association (C) and dissociation (D) time course of $[^3\text{H}]$ JNJ-54232334 on rat cortex homogenates. Data are expressed as mean \pm S.E.M. from 4 replicates per data point.

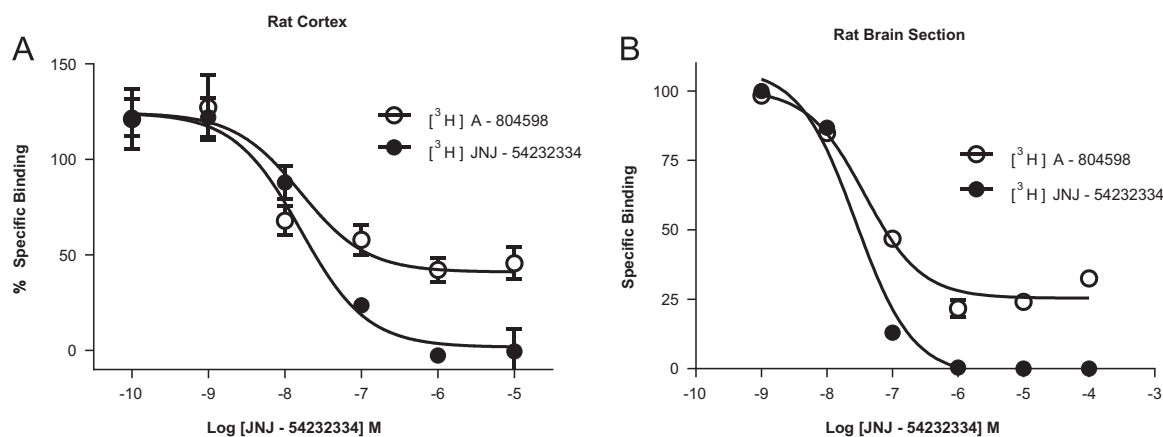


Fig. 5. Displacement of $[^3\text{H}]$ JNJ-54232334 and $[^3\text{H}]$ A-804598 in rat cortex homogenates with JNJ-54232334 (A). Displacement of $[^3\text{H}]$ JNJ-54232334 and $[^3\text{H}]$ A-804598 with JNJ-54140515 in rat brain sections (hippocampus). Data are expressed as mean \pm S.E.M. from 3–6 replicates per data point.

demonstrating the high non-specific binding observed in the hippocampus with $[^3\text{H}]$ A-804598. $[^3\text{H}]$ A-804598 exhibited similar non-specific signal in the P2X7 KO mouse (Fig. 7) with radioligand binding present in the hippocampus. These data collectively suggest that A-804598 binds to a site that is independent of P2X7 pharmacology. Another important feature of JNJ-54232334 binding in brain tissue sections, both in rats and mice, was the overall uniform and homogeneous binding.

3.3. P2X7 distribution with immunohistochemistry

We looked into the distribution of P2X7 in rat brain section using immunohistochemistry and as shown in Fig. 8, P2X7 is uniformly distributed throughout the brain. In this study, we show that P2X7 immuno-reactivity co-localized with microglial cell population (Fig. 8C; lower panel; bottom right). It is also evident from the merge picture that there is also a significant proportion of P2X7 expression in cell types not expressing Iba1, which is probably representative of different glial cells, notably astrocytes.

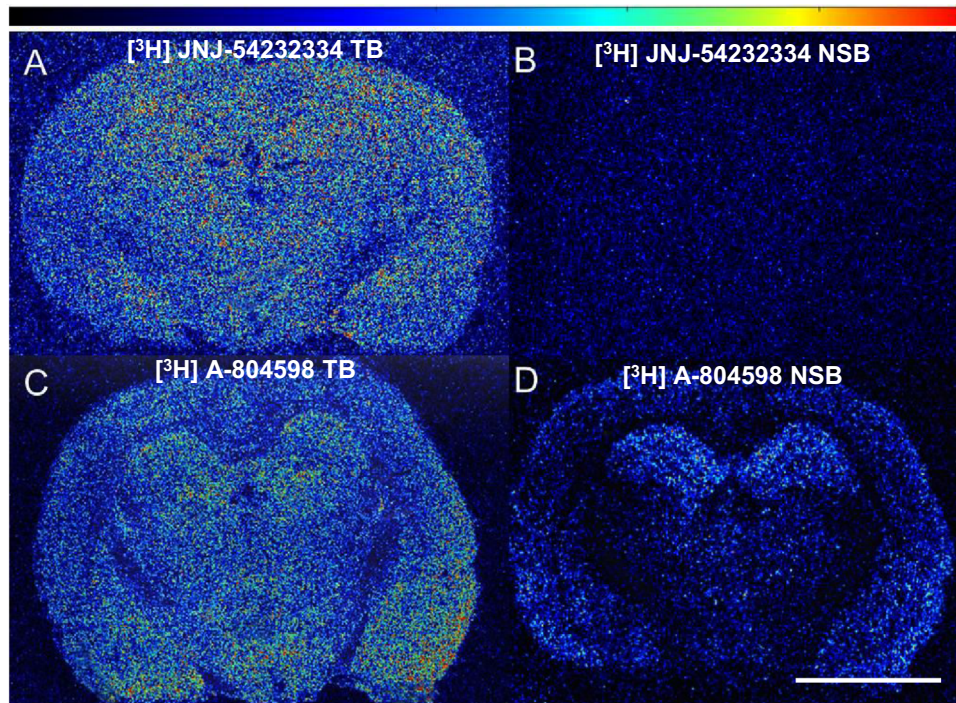


Fig. 6. Representative images of naïve control rats at the level of the hippocampus comparing 10 nM [^3H] JNJ-54232334 or 30 nM [^3H] JNJ-A-804598. (A) [^3H] JNJ-54232334 total binding (B) [^3H] JNJ-54232334 nonspecific binding in the presence of 10 μM MA-740003 (C) [^3H] JNJ-A-804598 total binding (D) [^3H] JNJ-A-804598 nonspecific binding in the presence of 100 μM A-740003. Note expression of [^3H] A-805498 in hippocampus of panel D. Images captured with β -Imager DFine. Scale bar, 5 mm.

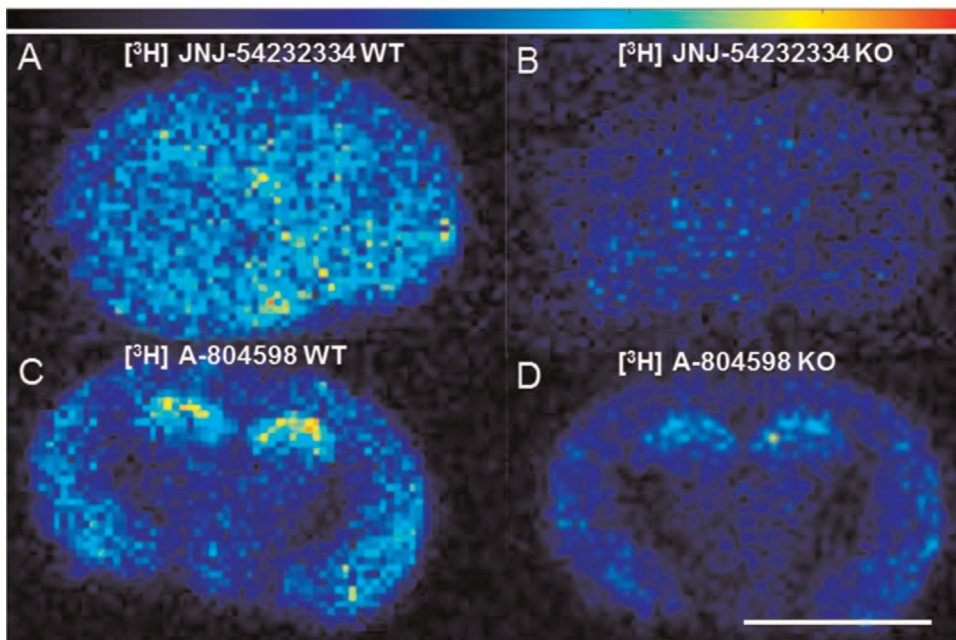


Fig. 7. Representative in vitro autoradiography images at the level of the hippocampus in the P2X7 WT and KO mouse. 10 nM [^3H] JNJ-54232334 in P2X7 WT mouse section (A), 10 nM [^3H] JNJ-54232334 in P2X7 KO mouse section (B), 30 nM [^3H] JNJ-A-804598 P2X7 WT mouse section (C), 30 nM [^3H] JNJ-A-804598 P2X7 KO mouse section (D). Note expression of [^3H] A-805498 in hippocampus of panel D. Images acquired with β -Imager TRacer. Scale bar, 5 mm.

3.4. Ex vivo receptor occupancy

Levels of P2X7 occupancy obtained after s.c. (time course) or p.o. (dose dependent) administration of JNJ-54140515 were measured using [^3H] JNJ-54232334 or [^3H] A-804598. A 10 mg/kg s.c. dose of JNJ-54140515 time dependently inhibited both [^3H] JNJ-54232334 and [^3H] A-804598 binding (Fig. 9A). Level of P2X7 occupancy measured with [^3H] A-804598 were $\sim 15\%$ lower at each time point compared to the levels obtained with [^3H] JNJ-

54232334 (Fig. 9A). Following the dose dependent experiment, a shift in ED_{50} of JNJ-54140515 was noted (Fig. 9B); using [^3H] JNJ-54232334 as the tracer, the ED_{50} of JNJ-54140515 was estimated at 0.8 mg/kg whereas the ED_{50} was 1.4 mg/kg on adjacent tissue sections incubated with [^3H] A-804598 (Fig. 9B). The mean non-specific binding of [^3H] A-804598 accounted for $\sim 42\%$ of the total binding whereas the non-specific binding with [^3H] JNJ-54232334 accounted for $\sim 16\%$ of the total binding for these experiments.

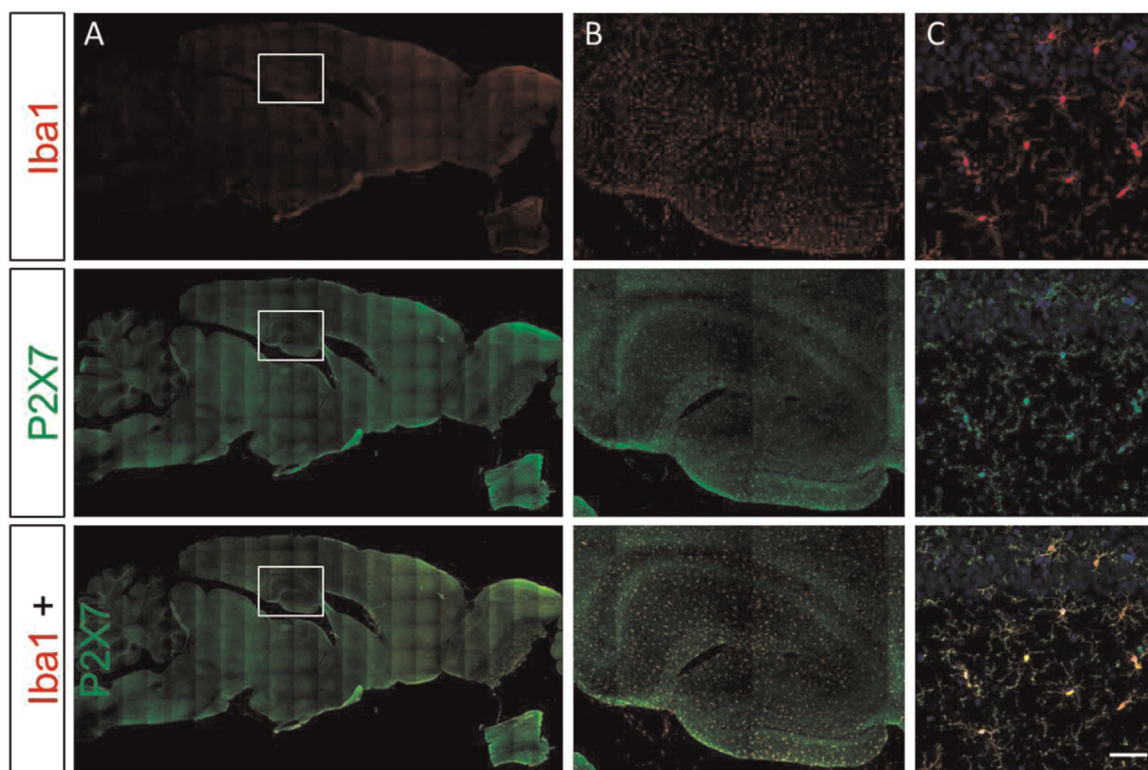


Fig. 8. Representative images showing P2X7 (green; middle panel) and Iba1 (red; upper panel) expression in the adult rat brain (A), zooming on the hippocampal region (white box) (B) and on the CA1 region (C). The lower panel is a merge of P2X7 and Iba1 staining to demonstrate co-localization of P2X7 with Iba1 expressing cells (microglia). Scale bar, 50 μm . (For interpretation of the references to color in this figure legend, the reader is referred to the web version of this article.)

4. Discussion

In the present study we characterize a new P2X7 radioligand [^3H] JNJ-54232334 and compared its properties to the previously described radioligand [^3H] A-804598. We demonstrate that this new radioligand has improved properties.

Radioligand binding is a key pharmacological assay in CNS drug discovery programs, particularly during the lead optimization phase. Radioligand binding is a unique assay as it offers the direct interpretation of ligand-receptor interaction, often in equilibrium, leading to estimates of affinity, a parameter used routinely to understand the amount of compound needed to bind half of the receptors (Hulme and Trevethick, 2010). As such most drug discovery programs either rely on prior radioligands (such as [^3H] A-804598), or discover improved radioligands (such as [^3H] JNJ-54232334) in the course of the discovery program. While [^3H] A-804598 provided a much needed tool to assess affinity at the recombinant P2X7 channel overexpressed in cell systems (such as rP2X7-1321N1 cells), [^3H] A-804598 is less than ideal for probing P2X7 in native systems. As we have described, [^3H] A-804598 binding cannot be completely displaced by P2X7 selective ligands, leading us to hypothesize that [^3H] A-804598 binds to a non-P2X7 site as well in native tissues.

Often lack of complete displacement indicates a novel binding site of the test compound and partial displacement of a radioligand is used as a first-pass fingerprint of allosterism. We do not believe that allosterism is in play here for the following reasons: (a) both [^3H] A-804598 and [^3H] JNJ-54232334 can be displaced by Bz-ATP (data not shown), albeit maximal displacement differs with Bz-ATP displacing [^3H] JNJ-54232334 more effectively than [^3H] A-804598 and, (b) in recombinant systems where P2X7 is expressed in 1321N1 cells, JNJ-54232334 (and all other compounds that we have tested, in excess of hundreds) displaced [^3H] A-804598 completely. Lack of complete displacement of [^3H]

A-804598 only happens in native brain tissue which indicates that [^3H] A-804598 binds to a non-P2X7 site. Clearly, [^3H] JNJ-54232334 does not share the similar non-P2X7 site as A-804598 and was clean in Eurofins selectivity panel at (> 50% inhibition at 1 μM) against a panel of 50 other neurotransmitter and neuropeptide receptors, and a panel of 65 kinases (data not shown). Even though A-804598 was shown to be a very selective compound (Donnelly-Roberts et al., 2009), selectivity for a compound is relative and can only be assessed for the targets available in the panel. It is clear that A-804598 binds to a different site other than P2X7. Our data obtained in P2X7 knockout brain sections clearly demonstrated that [^3H] A-804598 binds to a non-P2X7 binding site particularly abundant in the hippocampus.

Immunohistochemistry and in situ hybridization has shown the distribution of P2X7 receptors in rodent brain is widespread residing in wide range of glial cell types in the brain (Yu et al., 2008). Our autoradiography data are in agreement with Able et al. (2011) that represented P2X7 expression on microglia and astrocytes. However, [^3H] JNJ-54232334 exhibits a more uniform distribution pattern than [^3H] A-804598 in the rodent brain. With [^3H] JNJ-54232334 we did not observe high regional specificity that was reported with [^3H] A-804598 by Able et al. (2011). As we have shown, [^3H] A-804598 has a high degree of non-specific binding, especially in the hippocampus. When using specific brain regions to quantify the level of receptor occupancy with [^3H] A-804598, we noticed a decrease in signal to noise of the assay and a further underestimation of receptor occupancy compared to [^3H] JNJ-54232334 (data not shown). Although there is evidence of neuronal P2X7 expression (Alloisio et al., 2008; Diaz-Hernandez et al., 2008) our data suggest that the distribution of P2X7 is more ubiquitous as shown with our immunohistochemistry and autoradiography data with [^3H] JNJ-54232334.

Our new tracer [^3H] JNJ-54232334 was also suitable for the ex vivo autoradiography method. The ex vivo autoradiography

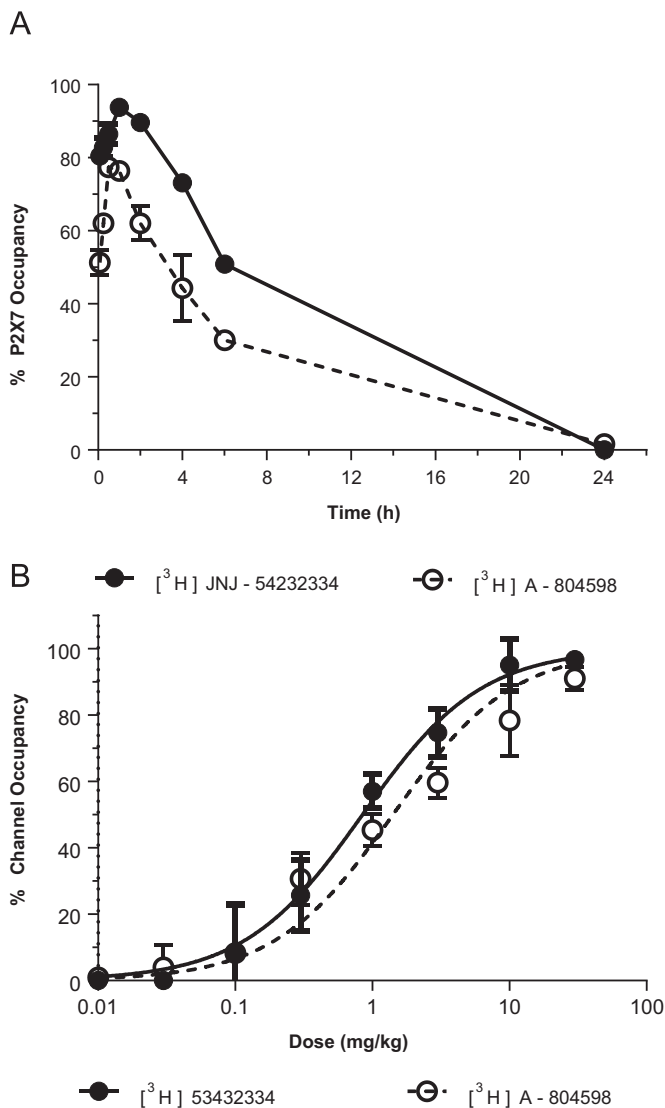


Fig. 9. Level of P2X7 ex vivo occupancy following p.o. or s.c. administration of JNJ-54140515 as measured in rat brain sections by ex vivo receptor autoradiography using [³H] JNJ-54232334 or [³H] A-804598. Time dependency of P2X7 occupancy following a 10 mg/kg s.c. dose of JNJ-54140515, (A). Dose dependency of P2X7 occupancy after p.o. administration of JNJ-54140515 measured 30 min after drug administration (B). Data in A and B are shown as the mean of three replicates per time point or dose \pm S.E.M.

technique is used to demonstrate P2X7 receptor occupancy, duration of occupancy and calculation of ED₅₀, as shown for JNJ-54140515. JNJ-54140515 was chosen over unlabeled JNJ-54232334 for receptor occupancy experiments due to a 10-fold increase in brain penetration while sharing similar in vitro affinity and potency. With JNJ-54140515, we observed a shift of potency between both tracers and this shift can influence decision making in drug discovery programs. [³H] JNJ-54232334 was superior to [³H] A-804598 in estimating occupancy, primarily due to reduced non-specific binding of [³H] JNJ-54232334. We have already demonstrated that [³H] A-804598 binds to sites that are resistant to displacement by P2X7 selective ligands; in contrast, [³H] JNJ-54232334 binding was completely displaced by the same set of ligands. This is probably the main reason behind the reduced non-specific binding obtained for [³H] JNJ-54232334. Reduction in non-specific binding was also achieved by decreasing the incubation time for ex vivo autoradiography from 10 min to 1 min and the importance of short incubation time given the unknown properties of novel compounds at the drug receptor complex has been

discussed previously by Langlois et al. (2001). Given the fast off-rate of JNJ-54232334 (and probably of JNJ-54140515 due to structural similarity), it is also possible that improved ex vivo autoradiography was aided by the shortened incubation time.

In closing, we have presented data highlighting JNJ-54232334 and JNJ-54140515 as high affinity P2X7 antagonists. We show evidence that [³H] JNJ-54232334 offers advantages over [³H] A-804598 as a radiotracer ligand for P2X7. We also found widespread and homogenous distribution of P2X7 autoradiography and immunohistochemistry in rat brain sections. P2X7 is expressed throughout the brain in a region independent manner; although the channel is ubiquitously expressed throughout the brain regions, it is only activated and functional under high concentrations (high μ M and/or low mM) of ATP, that is associated with cellular stress and necrosis (i.e. in pathological situations). JNJ-54232334 and JNJ-54140515 may offer insights to probe the role of P2X7 in various CNS diseases including neuropsychiatric and neurodegenerative disorders.

References

- Abdi, M.H., Beswick, P.J., Billinton, A., Chambers, L.J., Charlton, A., Collins, S.D., Collis, K.L., Dean, D.K., Fonfria, E., Gleave, R.J., Lejeune, C.L., Livermore, D.G., Medhurst, S.J., Michel, A.D., Moses, A.P., Page, L., Patel, S., Roman, S.A., Senger, S., Slingsby, B., Steadman, J.G., Stevens, A.J., Walter, D.S., 2010. Discovery and structure-activity relationships of a series of pyroglutamic acid amide antagonists of the P2X7 receptor. *Bioorg. Med. Chem. Lett.* 20, 5080–5084.
- Able, S.L., Fish, R.L., Bye, H., Booth, L., Logan, Y.R., Nathaniel, C., Hayter, P., Katugampola, S.D., 2011. Receptor localization, native tissue binding and ex vivo occupancy for centrally penetrant P2X7 antagonists in the rat. *Br. J. Pharmacol.* 162, 405–414.
- Alloisio, S., Cervetto, C., Passalacqua, M., Barbieri, R., Maura, G., Nobile, M., Marcoli, M., 2008. Functional evidence for presynaptic P2X7 receptors in adult rat cerebellar nerve terminals. *FEBS Lett.* 582, 3948–3953.
- Bartlett, R., Stokes, L., Sluyter, R., 2014. The P2X7 receptor channel: recent developments and the use of P2X7 antagonists in models of disease. *Pharmacol. Rev.* 66, 638–675.
- Basso, A.M., Bratcher, N.A., Harris, R.R., Jarvis, M.F., Decker, M.W., Rueter, L.E., 2009. Behavioral profile of P2X7 receptor knockout mice in animal models of depression and anxiety: relevance for neuropsychiatric disorders. *Behav. Brain Res.* 198, 83–90.
- Bhattacharya, A., Wang, Q., Ao, H., Shoblock, J.R., Lord, B., Aluisio, L., Fraser, I., Nepomuceno, D., Neff, R.A., Welty, N., Lovenberg, T.W., Bonaventure, P., Wickenden, A.D., Letavic, M.A., 2013. Pharmacological characterization of a novel centrally permeable P2X7 receptor antagonist: JNJ-47965567. *Br. J. Pharmacol.* 170, 624–640.
- Boucher, A.A., Arnold, J.C., Hunt, G.E., Spiro, A., Spencer, J., Brown, C., McGregor, I.S., Bennett, M.R., Kassiou, M., 2011. Resilience and reduced c-Fos expression in P2X7 receptor knockout mice exposed to repeated forced swim test. *Neuroscience* 189, 170–177.
- Chataigneau, T., Lemoine, D., Grutter, T., 2013. Exploring the ATP-binding site of P2X7 receptors. *Front. Cell. Neurosci.* 7, 273.
- Chrovian, C.C., Rech, J.C., Bhattacharya, A., Letavic, M.A., 2014. P2X7 antagonists as potential therapeutic agents for the treatment of CNS disorders. *Prog. Med. Chem.* 53, 65–100.
- Csolle, C., Ando, R.D., Kittel, A., Goloncser, F., Baranyi, M., Soproni, K., Zelena, D., Haller, J., Nemeth, T., Mocsai, A., Sperlagh, B., 2013a. The absence of P2X7 receptors (P2rx7) on non-haematopoietic cells leads to selective alteration in mood-related behaviour with dysregulated gene expression and stress reactivity in mice. *Int. J. Neuropsychopharmacol.* 16, 213–233.
- Csolle, C., Baranyi, M., Zsilla, G., Kittel, A., Goloncser, F., Illes, P., Papp, E., Vizi, E.S., Sperlagh, B., 2013b. Neurochemical changes in the mouse hippocampus underlying the antidepressant effect of genetic deletion of P2X7 receptors. *PLoS One* 8, 1–18.
- Diaz-Hernandez, M., Del Puerto, A., Diaz-Hernandez, J.I., Diez-Zaera, M., Lucas, J.J., Garrido, J.J., Miras-Portugal, M.T., 2008. Inhibition of the ATP-gated P2X7 receptor promotes axonal growth and branching in cultured hippocampal neurons. *J. Cell Sci.* 121, 3717–3728.
- Donnelly-Roberts, D.L., Namovic, M.T., Surber, B., Vaidyanathan, S.X., Perez-Medrano, A., Wang, Y., Carroll, W.A., Jarvis, M.F., 2009. [(3H)A-804598] [(3H)2-cyano-1-[(15)-1-phenylethyl]-3-quinolin-5-ylguanidine] is a novel, potent, and selective antagonist radioligand for P2X7 receptors. *Neuropharmacology* 56, 223–229.
- Gao, M., Wang, M., Green, M.A., Hutchins, G.D., Zheng, Q.H., 2015. Synthesis of [(11)C]GSK1482160 as a new PET agent for targeting P2X7 receptor. *Bioorg. Med. Chem. Lett.* 25, 1965–1970.
- Goshen, I., Kreisel, T., Ben-Menachem-Zidon, O., Licht, T., Weidenfeld, J., Ben-Hur, T., Yirmiya, R., 2008. Brain interleukin-1 mediates chronic stress-induced

- depression in mice via adrenocortical activation and hippocampal neurogenesis suppression. *Mol. Psychiatry* 13, 717–728.
- Gubert, C., Fries, G.R., Pfaffenseller, B., Ferrari, P., Coutinho-Silva, R., Morrone, F.B., Kapczinski, F., Battastini, A.M., 2014. Role of P2X7 receptor in an animal model of mania induced by D-amphetamine. *Mol. Neurobiol.* [PMID: 25502294]
- Hulme, E.C., Trevethick, M.A., 2010. Ligand binding assays at equilibrium: validation and interpretation. *Br. J. Pharmacol.* 161, 1219–1237.
- Iwata, M., Ota, K.T., Duman, R.S., 2013. The inflammasome: pathways linking psychological stress, depression, and systemic illnesses. *Brain Behav. Immun.* 31, 105–114.
- Koo, J.W., Duman, R.S., 2008. IL-1 β is an essential mediator of the antineurogenic and anhedonic effects of stress. *Proc. Natl. Acad. Sci. USA* 105, 751–756.
- Langlois, X., te Riele, P., Wintmolders, C., Leysen, J.E., Jurzak, M., 2001. Use of the beta-imager for rapid ex vivo autoradiography exemplified with central nervous system penetrating neurokinin 3 antagonists. *J. Pharmacol. Exp. Ther.* 299, 712–717.
- Letavic, M.A., Lord, B., Bischoff, F., Hawryluk, N.A., Pieters, S., Rech, J.C., Sales, Z., Velter, A.I., Ao, H., Bonaventure, P., Contreras, V., Jiang, X., Morton, K.L., Scott, B., Wang, Q., Wickenden, A.D., Carruthers, N.I., Bhattacharya, A., 2013. Synthesis and pharmacological characterization of two novel, brain penetrating P2X7 antagonists. *ACS Med. Chem. Lett.* 4, 419–422.
- Lord, B., Aluisio, L., Shoblock, J.R., Neff, R.A., Varlinskaya, E.I., Ceusters, M., Lovenberg, T.W., Carruthers, N., Bonaventure, P., Letavic, M.A., Deak, T., Drinkenburg, W., Bhattacharya, A., 2014. Pharmacology of a novel central nervous system-penetrant P2X7 antagonist JNJ-42253432. *J. Pharmacol. Exp. Ther.* 351, 628–641.
- Ortiz, R., Ulrich, H., Zarate Jr., C.A., Machado-Vieira, R., 2015. Purinergic system dysfunction in mood disorders: a key target for developing improved therapeutics. *Prog. Neuropsychopharmacol. Biol. Psychiatry* 57, 117–131.
- Rudolph, D.A., Alcazar, J., Ameriks, M.K., Anton, A.B., Ao, H., Bonaventure, P., Carruthers, N.I., Chrovian, C.C., De Angelis, M., Lord, B., Rech, J.C., Wang, Q., Bhattacharya, A., Andres, J.I., Letavic, M.A., 2015. Novel methyl substituted 1-(5,6-dihydro-[1,2,4]triazolo[4,3-a]pyrazin-7(8H)-yl)methanones are P2X7 antagonists. *Bioorg. Med. Chem. Lett.* 25, 3157–3163.
- Savall, B.M., Wu, D., De Angelis, M., Carruthers, N.I., Ao, H., Wang, Q., Lord, B., Bhattacharya, A., Letavic, M.A., 2015. Synthesis, SAR, and pharmacological characterization of brain penetrant P2X7 receptor antagonists. *ACS Med. Chem. Lett.* 6, 671–676.
- Solle, M., Labasi, J., Perregaux, D.G., Stam, E., Petrushova, N., Koller, B.H., Griffiths, R. J., Gabel, C.A., 2001. Altered cytokine production in mice lacking P2X(7) receptors. *J. Biol. Chem.* 276, 125–132.
- Sperlagh, B., Csolle, C., Ando, R.D., Goloncser, F., Kittel, A., Baranyi, M., 2012. The role of purinergic signaling in depressive disorders. *Neuropsychopharmacol. Hung.: Magyar Pszichofarmakologiai Egyesulet lapja (Off. J. Hung. Assoc. Psychopharmacol.)* 14, 231–238.
- Sperlagh, B., Illes, P., 2014. P2X7 receptor: an emerging target in central nervous system diseases. *Trends Pharmacol. Sci.* 35, 537–547.
- Stokes, L., Spencer, S.J., Jenkins, T.A., 2015. Understanding the role of P2X7 in affective disorders—are glial cells the major players? *Front. Cell. Neurosci.* 9, 258.
- Wilkinson, S.M., Gunosewoyo, H., Barron, M.L., Boucher, A., McDonnell, M., Turner, P., Morrison, D.E., Bennett, M.R., McGregor, I.S., Rendina, L.M., Kassiou, M., 2014. The first CNS-active carborane: a novel P2X7 receptor antagonist with antidepressant activity. *ACS Chem. Neurosci.* 5, 335–339.
- Yu, Y., Ugawa, S., Ueda, T., Ishida, Y., Inoue, K., Kyaw Nyunt, A., Umemura, A., Mase, M., Yamada, K., Shimada, S., 2008. Cellular localization of P2X7 receptor mRNA in the rat brain. *Brain Res.* 1194, 45–55.
- Zhang, Y., Liu, L., Liu, Y.Z., Shen, X.L., Wu, T.Y., Zhang, T., Wang, W., Wang, Y.X., Jiang, C.L., 2015. NLRP3 inflammasome mediates chronic mild stress-induced depression in mice via neuroinflammation. *Int. J. Neuropsychopharmacol.* 8, 1–8.